

Verifying the ACIS Contamination Model with 1E0102.2-7219

J. M. DePasquale, P. P. Plucinsky, A. A. Vikhlinin, R. J. Edgar ▶ Harvard-Smithsonian Center for Astrophysics 🌐
H. L. Marshall, N. S. Schultz ▶ MIT Center for Space Research

I. Abstract & Introduction

The low-energy sensitivity of the ACIS instrument has been continuously degrading over the last 4 years due to the accumulation of a layer of contamination on the ACIS filter and/or CCDs. This contamination layer, the result of outgassing within the telescope, introduces a new, energy dependent absorption into the ACIS response. The thickness of this layer has been increasing with time and its spatial distribution across the ACIS focal plane has been continually changing with time. We utilize multiple observations of the SMC Supernova Remnant 1E0102.2-7219 to verify the models for the spectral, temporal and spatial dependence of the contamination layer. 1E0102.2-7219 has a soft, line-dominated spectrum which is very sensitive to the additional absorption of the contamination layer. The extensive calibration observations of 1E0102.2-7219 over the course of the mission at several different locations on the ACIS I and S arrays make this source an ideal laboratory for verifying the temporal and spatial dependence of the contamination model.

II. Spectral Processing

This analysis includes all observations of E0102 on the I3 chip; Table 1 summarizes all 31 observations. We begin processing by running CTI correction via *acis_process_events* on the level 1 events file and subsequently filtering on good grades, gti and chip number to create the level 2 events file. *apply_gain* is then applied to the level 2 events file to adjust for time-dependent PI channel gain. *acisspec* is used to extract the spectrum in PI with the source and background regions defined in DS9. Once spectral extraction is complete, *calcrmf2* and *calcarf* are run to compute the new weighted rmf and arf files which incorporate the spatial and time dependent contamination model. The default, weighted rmf and arf created during extraction are used to compare the test results to the default results. This exact processing sequence was performed on all 31 E0102 observations prior to the analysis. Please refer to Figure 1 for a flow chart of this processing.

Obsid	Date (DOY)	Y offset	Z offset
0440	2000-04-04	-0.5	2.5
0439	2000-04-04	-2.25	2.5
0136	2000-03-16	-4.0	2.5
0140	2000-04-04	-5.5	2.5
0420	2000-03-14	-7.0	2.5
1313	2000-12-15	-7.0	0.5
1314	2000-12-15	-4.0	0.5
1315	2000-12-15	-4.0	2.5
1316	2000-12-15	-4.0	4.5
1317	2000-12-15	-4.0	6.5
1533	2001-06-05	-7.0	0.5
1534	2001-06-05	-4.0	0.5
1535	2001-06-05	-4.0	2.5
1536	2001-06-05	-4.0	4.5
1537	2001-06-05	-4.0	6.5
2835	2001-12-05	-7.0	0.5
2836	2001-12-05	-4.0	0.5
2837	2001-12-05	-4.0	2.5
2838	2001-12-05	-4.0	4.5
2839	2001-12-05	-4.0	6.5
2857	2002-06-21	-7.0	0.5
2858	2002-06-21	-4.0	0.5
2859	2002-06-21	-4.0	2.5
2860	2002-06-21	-4.0	4.5
2861	2002-06-21	-4.0	6.5
3533	2003-02-01	-7.0	0.5
3536	2003-02-02	-4.0	0.5
3537	2003-02-02	-0.5	0.5
3526	2003-08-06	-7.0	0.5
3527	2003-08-07	-4.0	0.5
3528	2003-08-09	-0.5	0.5

Table 1:
E0102 I3 observations

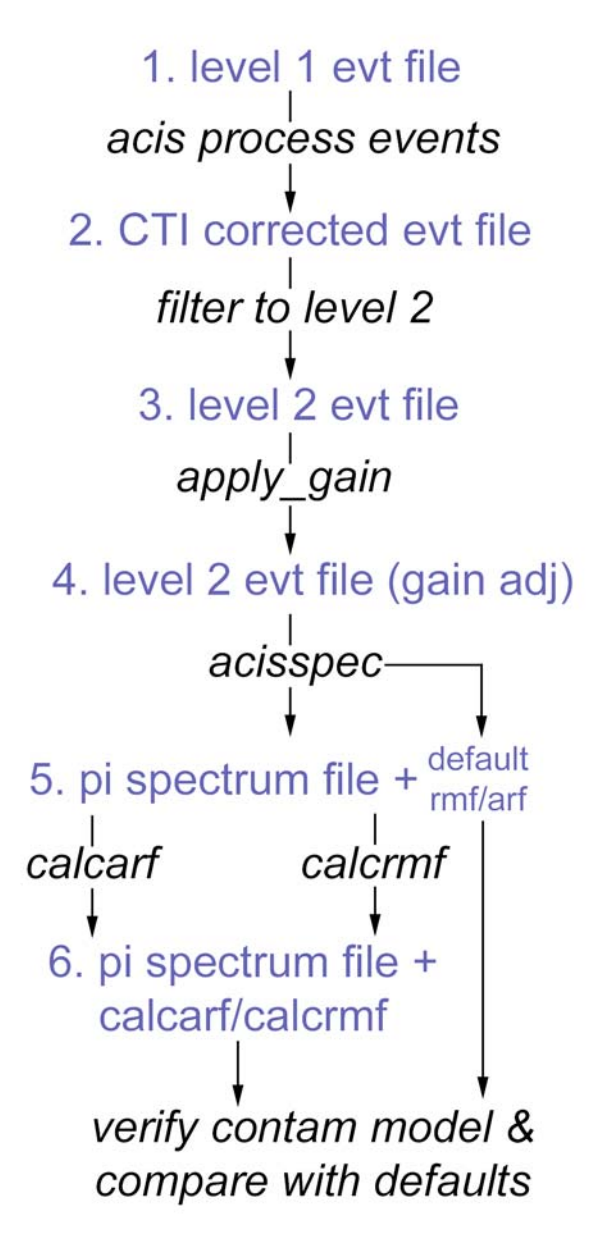
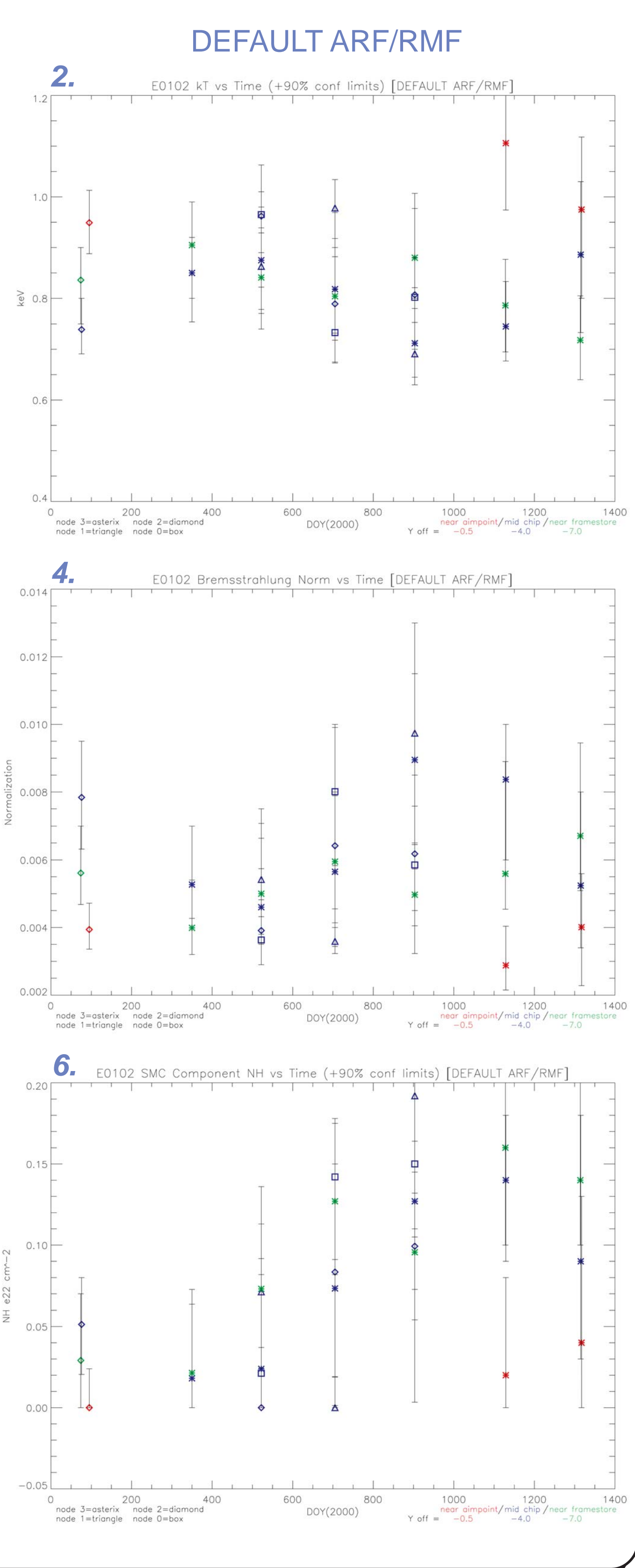
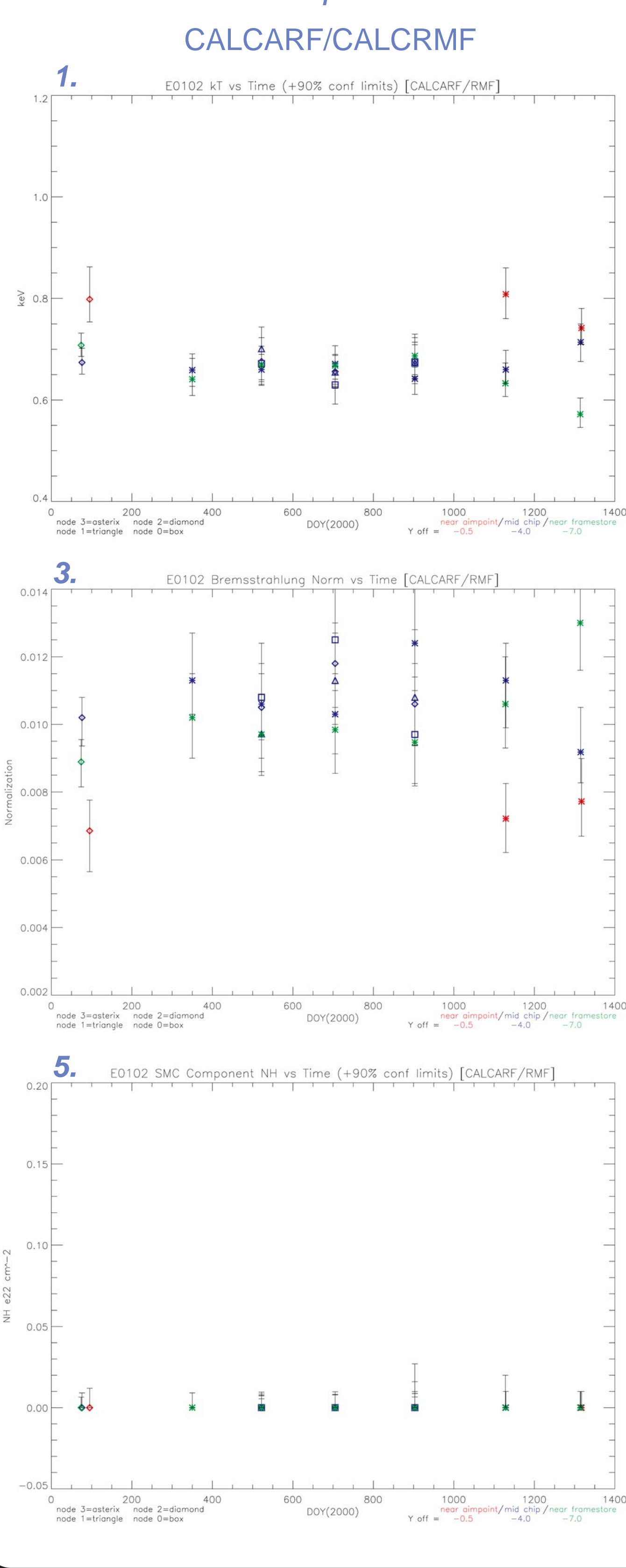


Figure 1:
processing flow chart

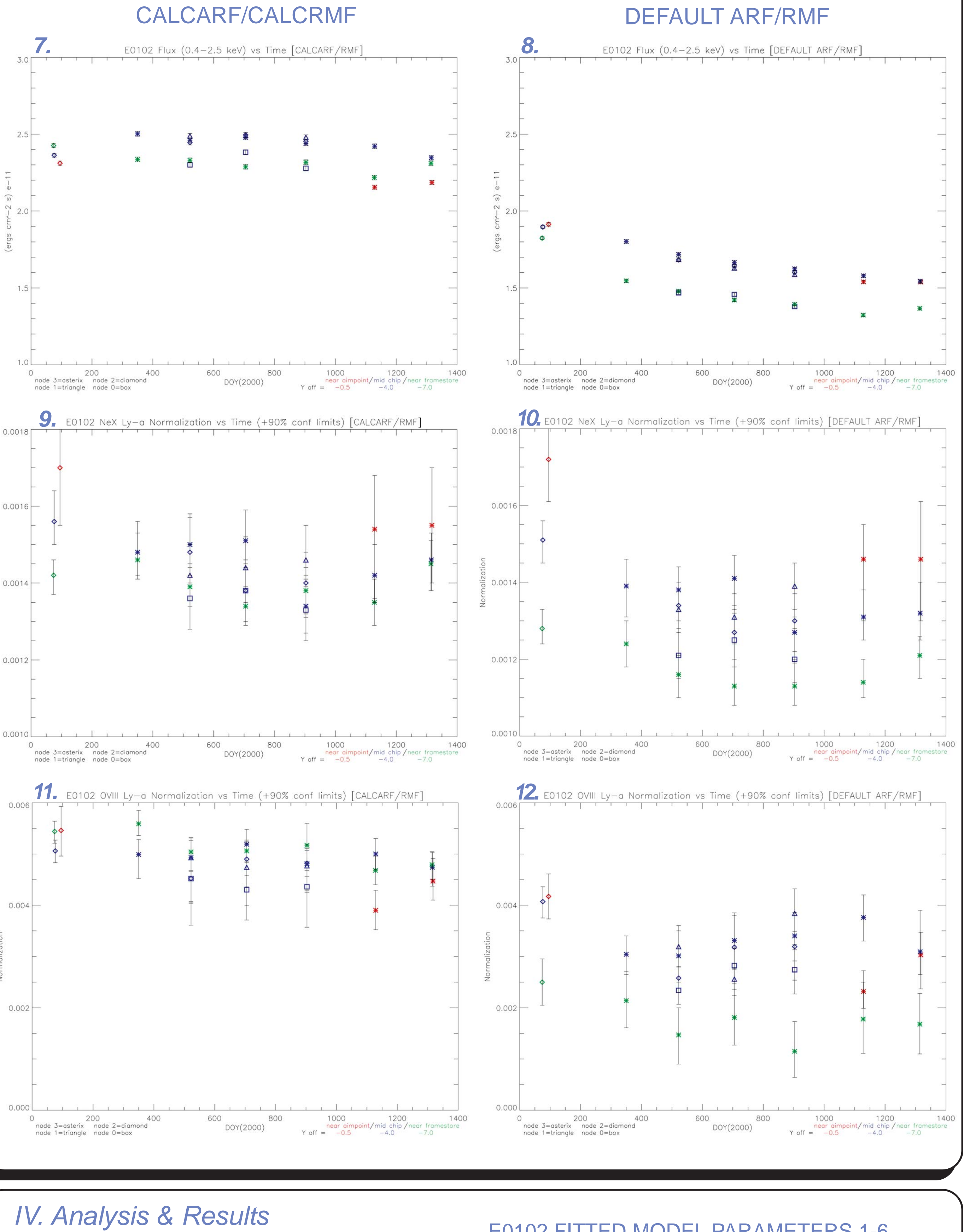
λ (Å)	Energy (keV)	Line Description	T Peak	Peak Emissivity/Emissivity (K)	photon cm ⁻² s ⁻¹
22.100	0.7	0.7 $1s^2(S_0) - 1s2p^2(P_1)$ [Re]	2.0×10^6	3.52×10^{-15}	7.7×10^{-18}
21.600	0.574	0.7 $1s^2(S_0) - 1s2p^2(P_1)$ [Re]	2.0×10^6	3.43×10^{-15}	7.4×10^{-18}
18.090	0.665	0.7 $1s^2(S_0) - 1s2p^2(P_1)$ [Ly α]	2.0×10^6	3.74×10^{-16}	7.0×10^{-19}
18.627	0.665	0.7 $1s^2(S_0) - 1s2p^2(P_1)$ [Ly α]	2.0×10^6	3.43×10^{-16}	6.7×10^{-19}
17.770	0.698	0.7 $1s^2(S_0) - 1s2p^2(P_1)$	2.5×10^6	9.82×10^{-17}	2.2×10^{-19}
16.090	0.712	0.7 $1s^2(S_0) - 1s2p^2(P_1)$ [Ly α]	2.0×10^6	3.08×10^{-16}	6.8×10^{-19}
15.180	0.817	0.8 $1s^2(S_0) - 3p^2(P_{3/2})$ [Ly β]	3.16×10^6	1.20×10^{-16}	3.0×10^{-19}
14.821	0.817	0.8 $1s^2(S_0) - 3p^2(P_{3/2})$ [Ly β]	3.16×10^6	5.24×10^{-16}	1.4×10^{-19}
13.720	0.817	0.8 $1s^2(S_0) - 3p^2(P_{3/2})$ [Re]	3.08×10^6	3.00×10^{-16}	8.5×10^{-20}
13.447	0.923	Net $1s^2(S_0) - 1s2p^2(P_1)$ [Re]	3.08×10^6	4.11×10^{-16}	1.0×10^{-19}
12.135	0.923	Net $1s^2(S_0) - 1s2p^2(P_1)$ [Re]	3.08×10^6	3.80×10^{-16}	9.5×10^{-20}
11.560	1.073	Net $1s^2(S_0) - 1s2p^2(P_1)$ [Ly α]	3.08×10^6	4.79×10^{-17}	1.0×10^{-19}
11.000	1.127	Net $1s^2(S_0) - 1s2p^2(P_1)$ [Ly α]	3.08×10^6	1.25×10^{-17}	1.0×10^{-19}
10.750	1.127	Net $1s^2(S_0) - 1s2p^2(P_1)$ [Ly β]	3.08×10^6	5.05×10^{-17}	1.0×10^{-19}
10.239	1.212	Net $1s^2(S_0) - 3p^2(P_{3/2})$ [Ly β]	6.31×10^6	4.27×10^{-17}	1.0×10^{-19}
9.709	1.277	Net $1s^2(S_0) - 3p^2(P_{3/2})$ [Ly β]	6.31×10^6	4.38×10^{-17}	1.0×10^{-19}
9.213	1.322	Net $1s^2(S_0) - 3p^2(P_{3/2})$ [Ly β]	6.31×10^6	7.29×10^{-17}	1.0×10^{-19}
9.169	1.352	Mg II $1s^2(S_0) - 1s2p^2(P_1)$ [Re]	6.31×10^6	1.12×10^{-16}	1.0×10^{-19}
7.850	1.379	Mg II $1s^2(S_0) - 1s2p^2(P_1)$ [Re]	6.31×10^6	1.31×10^{-17}	1.0×10^{-19}
7.310	1.696	Mg II $1s^2(S_0) - 1s2p^2(P_1)$ [Ly α]	6.31×10^6	1.38×10^{-18}	1.0×10^{-19}
6.183	2.006	S III $1s^2(S_0) - 3p^2(P_{3/2})$ [Ly α]	1.58×10^8	4.95×10^{-17}	1.0×10^{-19}
5.218	2.375	S III $1s^2(S_0) - 3p^2(P_{3/2})$ [Ly β]	1.58×10^8	6.80×10^{-18}	1.0×10^{-19}

Table 2:
E0102 spectral model included lines

E0102 fitted model parameters vs time



E0102 fitted model parameters vs time



IV. Analysis & Results

In analyzing the various E0102 I3 observations, each data set was loaded into *xspec* with the 1st and “bad” PI channels ignored to avoid undesirably influencing the fit. The spectral model was then loaded and fit to the data allowing the line energy normalizations to float, as well as the SMC component absorption, and the bremsstrahlung temperature and normalization. Please refer to Figure 2 for a sample fit of obsid 136. Please refer to figure 3 for an illustration of the I3 E0102 observations.

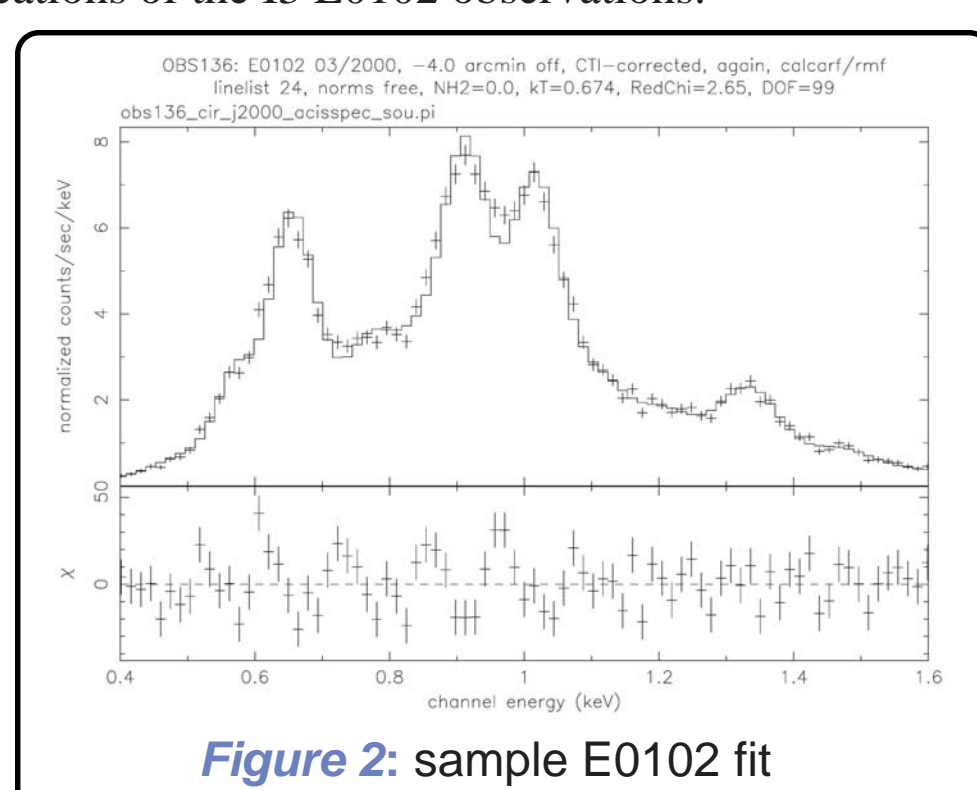


Figure 2: sample E0102 fit

Although all line energy normalizations were allowed to float in most cases, there were 3 obsids in which the 665 eV OVIII Ly α line was constrained to be 10% of the 654 eV OVIII Ly α line. These 3 cases were for observations taken near the I3 aim point, where CTI contributes to lower spectral resolution such that these two O lines are not resolved. Without this constraint, the spectral fit places too much flux in the 665 eV line, which artificially reduces the flux of the 654 eV line. These were obsids 440, 3437 and 3528 with Y-offsets of -0.5, -0.3 and -0.2 respectively. Once fitting was complete, *steppar* or *error* was used to find the 90% confidence error bars. Flux error was attained by evaluating the count rate/count rate error ratio to flux and flux error relationship.

Figure 3: ACIS I3 illustration

E0102 FITTED MODEL PARAMETERS 1-6

The differences between the calcarf/rmf fitted data and the default arf/rmf fitted data are immediately apparent, and dramatically illustrate spatial and time dependent effects of the contamination layer.

→ Notice in plots 1 and 2 that using calcarf/rmf greatly reduces the uncertainty in the bremsstrahlung temperature kT, as well as converges the spatial differences seen in the default fit results.

→ The bremsstrahlung normalization seen in plots 3 and 4 is consistently higher in the calcarf/rmf fits, indicating that the absorption by the contaminant has been accounted for.

→ The SMC component neutral Hydrogen column density in plots 5 and 6 exhibits a striking difference between the calcarf/rmf fits and the default arf/rmf fits. As would be expected, the default fits show the NH absorption continually increasing over time, presumably to account for increasing contaminant over time. Though the calcarf/rmf fits show a consistent NH absorption value over time, it is consistently 0, which may indicate an overall overcorrection of the contaminant absorption over time.

E0102 FITTED MODEL PARAMETERS 7-12

→ Plots 7 and 8 show the model flux from 0.4 to 2.5 keV. The calcarf/rmf results are again consistently higher than the default results. As one would expect, the default results show a decrease in flux over time, consistent with time-dependent absorption. This effect is mitigated by the contamination model, though it appears the model may underestimate the contaminant at later dates.

→ The NeX Ly α normalization vs time is shown in plots 9 and 10. The contamination model consistently increases the flux of this line over the default results, though it appears the model may not include enough contaminant on the middle of the chip, the “near aim point” results are slightly higher in normalization than expected. The results are largely consistent in time however, agreeing well with the contamination time dependence.